FACTA UNIVERSITATIS
Series: **Mechanics, Automatic Control and Robotics** Vol.3, N° 13, 2003, pp. 715 - 727

UNSTABLE FRACTURE BEHAVIOUR OF WELD METAL AT A HIGH STRENGTH LOW ALLOY STEEL

UDC 539.388.2 669.15-194.2

Nenad Gubeljak

University of Maribor, Faculty of Mechanical Engineering
Smetanova 17, SI-2000 Maribor, Slovenia

Abstract. *Local brittle zones (LBZ) cause the unstable fracture behaviour of weld metals. This threatens the safe service of welded structures and makes structural assessment procedures difficult. Therefore, the unstable fracture behaviour of an overmatched high strength low alloyed steel weldment was experimentally investigated. It shows that any interaction between two adjacent weld metal regions with different hardness (over-to-under matching regions) produces local brittle zones, causing local unstable fracture behaviour. The formation of a low hardness region is attributed to the multipass welding reheating process between Ac_1 and the self-tempering temperature. The presence of partly solid metallic inclusions with a high content of alloying elements and pro-eutectoid ferrite microstructure were found to be additional causes for the local unstable fracture behaviour of the weld metal. Local strength mis-match localized the yielding and strain hardening in the undermatched region of the weld metal, contributing significantly to unstable fracture behaviour. Thus, a significantly different scatter of experimental (fracture toughness testing) results can be obtained. In the cases of specimens with through-the-thickness crack, not only is the scatter significantly lower, but the toughness itself.*

Key words: *Fracture mechanics of welded joints, crack tip opening displacement, local brittle zones, pro-eutectoid ferrite, inclusions*

Nomenclature

A_t – maximum tensile elongation
a – crack length
a/W – relative length of crack
B – thickness of specimen
BM – base metal
CE – carbon equivalent
$CTOD$ – crack tip opening displacement
$CTOD$ – CTOD defined for a gauge length of 5mm
Cv – impact toughness of V-notched Charpy specimen
M – mis-match factor
$SENB$ – single edge notch bend specimen
WDS – Wave dispersion spectrometer analyses
WM – weld metal
WM_{fill} – weld metal in the filler region of weld metal
WM_{root} – weld metal in the root region of weld metal
α – ferrite phase
γ – austenite phase
σ_{yBM} – average yield stress of base metal
σ_{yWM} – average yield stress of weld metal

Received October 20, 2002

E – Young's modulus
$HV_{0.1}$ – Value of Vickers hardness
LBZ – local brittle zone
$\sigma_y(HV)$ – yield stress of weld metal calculated by using empirical relationship between the microhardness and yield stress

1. INTRODUCTION

High strength low alloy (HSLA) steel of grade HT 80 is used for light-weight structures to increase their loading capacity. Having in mind the shielding effect of strength overmatching on weldment fracture behaviour, designers are commonly using filler metals with higher yield strengths compared to a base metal, in order to produce such a weldment. On the other hand, such a weldment can be the critical one for structural integrity due to possible unstable fracture behaviour [1]. Using HSLA steel weldments ensures the high loading capacity of a structure but decreases elongation enabling failure by lower deformation ability rather than low strength steels. Therefore, the use HSLA steels is limited. The safe usage of HSLA steel welded structures requires complete fracture behaviour characterisation and determination of weld metals fracture resistance. The reasons for this are: high-low strength microstructure within the weld metal and the shaping of low strength primary ferrite regions. This paper describes the effect of strength heterogeneous regions of weld metals on the fracture behaviour and consequently on the safe service usage of a welded structure.

2. THE WELDMENT PROPERTIES AND MICROSTRUCTURE

Welding was done using flux cored arc process with 40 mm thick plates. The composition of the base and filler material (flux core wire), Table 1, was chosen to produce the overmatched welded joint [2]. The groove preparation and other welding procedure details are described elsewhere [3].

Tensile properties of the weld metal were obtained by the testing of round specimens (diameter $\phi 5$), taken in the welding direction, in accordance with DIN 50125, and presented in Tab. 2, together with the values for the strength mis-match factor, M, defined as the ratio between the weld metal and the base metal yield strength:

$$M = \frac{\sigma_{y,WM}}{\sigma_{y,BM}} \tag{1}$$

where the subscripts WM and BM denote the properties of the weld and base metal, respectively.

The difference between the all-weld metal and weld metal composition should take into account, due to dilution between the base and filler material, as evident from Tab. 1. In addition metallurgical processes during solidification are responsible for local yield and tensile strength changes in the weld metal. The lower yield strength and higher Charpy impact toughness values were obtained in the weld metal root region (WM_{root}) rather than in the filler and cap region (WM_{fill}), as shown in Fig. 1 and Tab. 1. The large range of impact toughness values in the transition temperature region, Fig. 1, should also be noticed, indicating possible large range in fracture toughness values.

The microhardness results, Fig. 2, show significant deviation along the weld metal centre line. This deviation indicates the presence of regions with low strength, even lower than the base metal. Interaction between these regions and the surrounding high strength regions (over-to-under matching region) leads to the formation of local brittle zones (LBZ), which, in turn, cause local unstable fracture behaviour, as explained later.

Table 1. Chemical composition of base metal, pure weld metal and the actual weld metal of the filler and the root region

Material	C %	Si %	Mn %	P %	S %	Cr %	Ni %	Mo %	CE %
Base metal	0.09	0.27	0.25	0.015	0.004	1.12	2.63	0.25	0.366
Weld metal (pure)	0.06	0.35	1.43	0.011	0.008	0.86	3.01	0.56	0.448
WM_{fill} (filler region)	0.07	0.33	1.27	0.008	0.006	0.86	2.21	0.47	0.404
WM_{root}(root region)	0.08	0.32	0.78	0.012	0.007	0.99	2.50	0.35	0.388

Table 2. Average values of tensile properties of the base metal and welded metal-WM

Material	Temp. °C	E GPa	$R_{P0.2}$ MPa	R_m MPa	A_t %	Cv^+ J	M
Base	20°	201	711	838	19.6	$54_{-40°C}$	–
metal	–10°	209	712	846	19	$85_{-10°C}$	–
WM	20°	210†	770	845	16	$56_{-10°C}$	(1.08)
WM_{fill}	20°	205	861	951	11.7	$56_{-10°C}$	1.21
	–10°	211	873	1041	10.8	$33_{-40°C}$	1.22
WM_{root}	20°	221	807	905	15.3	$61_{-10°C}$	1.14
	–10°	212	824	902	16.5	$50_{-40°C}$	1.16

$^+$-mean value of three Charpy-V notched impact toughness specimens (Fig. 1),
†- Value has been estimated because the accurate experimental value was not available.

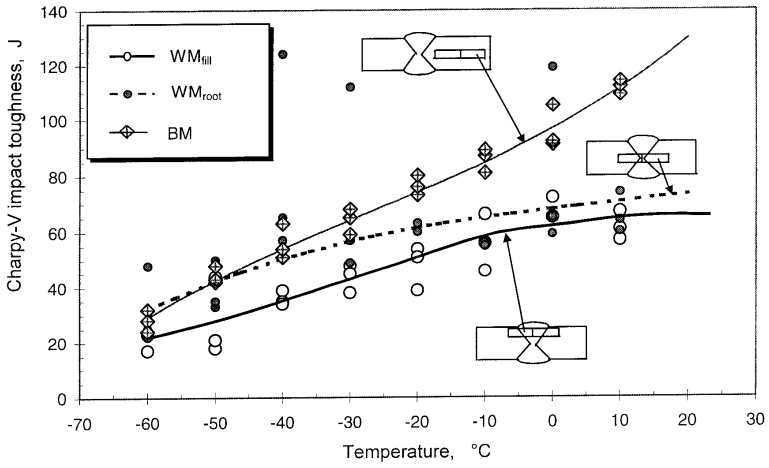

Fig. 1. Average and measured toughness vs. temperature curves for different weld metal regions and the base metal

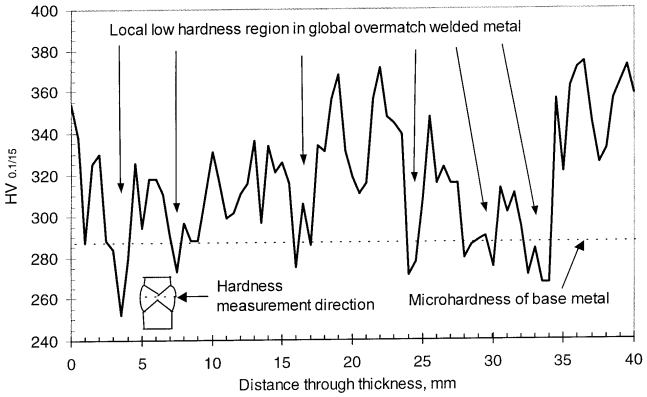

Fig. 2. Measurement of hardness in the through thickness of the weld joint

While the base metal microstructure consists of tempered martensite and upper bainite [4], the multipass weld metal, as described in [3], consists of more than one microstructure, as follows:

– re-heated fine grain martensite-bainite (close to the subsequent pass, exposed to the temperatures above Ac_1) with the highest hardness,
– as-deposited (columnar) bainite with contours of primary ferrite (away from the subsequent pass) with intermediate hardness:
  partially transformed microstructure (in-between previous two, relatively small iz size and not easily identified, exposed to the temperatures below Ac_1 and above self-tempering temperatures) with the lowest hardness.

3. RESULTS OF FRACTURE TOUGHNESS TESTING

The fracture testing was done on two types of specimens, one with a through-the-thickness crack (Bx2B) and the other with a surface crack (BxB), Figure 3, as according to standard [5]. While the first group of specimens had somewhat different crack lengths (a_0/W=0.19÷0.32), the second one had approximately the same crack length (a_0/W=0.48÷0.50). The crack tip opening displacement (CTOD) was considered to be the relevant fracture mechanic parameter [5]. The results for the CTOD values at crack growth initiation (δ_i) and at point of instability ($\delta_{c,u}$) are shown in Table 3, together with the values of the force at initiation (F_i) and at the maximum (F_{max}). The crack tip in BxB specimen was positioned in one of the two dominant microstructures, the re-heated one, denoted by WM(A) or the as-deposited one, denoted by WM(B).

In addition to the unstable fracture behaviour after the initial plastic deformation, [3], the main feature of BxB specimen testing was a strong dependence of fracture toughness on a microstructure ahead of the crack tip, indicated by at least two facts:

– The large scatter of (δ_i) and ($\delta_{c,u}$) values. Even if the specimen BxB-AD6 is excluded, the range of (δ_i) for the BxB-AD specimens is 0.045÷0.090 mm and the range of ($\delta_{c,u}$) is 0.102÷0.345 mm, while for the BxB-RH specimens the corresponding values are 0.135÷1.168 and 0.228÷0.561, respectively.
– The lower values of both (δ_i) and ($\delta_{c,u}$) are obtained for the as-deposited microstructure rather than for the re-heated microstructure.

To some extent, the (δ_i) and ($\delta_{c,u}$) values are also influenced by the crack length, since they decrease with crack length increase, but this is obviously of secondary importance and does not interfere with the microstructural effects [6].

The unstable fracture behaviour after initiation is even more pronounced for the Bx2B specimens, with the lower values for both (δ_i) and ($\delta_{c,u}$) than in the case of the BxB specimens. Furthermore, the main feature of Bx2B testing was the smaller scatter of (δ_i) and ($\delta_{c,u}$) values (especially the latter ones), indicating lower influence of microstructure. This is consistent with the fact that the crack tip encompasses all microstructures in the Bx2B specimens and does not cross one by one, as in the case of BxB specimens. Although longer crack length contributed somewhat to the generally lower fracture toughness obtained by Bx2B specimens as compared to the BxB specimens, it is obvious that the microstructure has the dominant role in creating this difference in the fracture behaviour of these two types of specimens.

In order to explain microstructural influence on fracture behaviour, metallographic and fractographic analyses were performed on both types of specimens.

4. FRACTOGRAPHIC AND METALLOGRAPHIC EXAMINATION

The fractographic examinations were performed by using a Scanning Electron Microscope (SEM), whilst the metallographic investigations were performed using an Optical Microscope (OM). Specimens Bx2B were cut perpendicularly to the crack growth direction as shown in Figure 3, whilst the specimens BxB were cut in the crack growth direction only, as shown on the right-hand side of Figure 3. The slices were polished and etched using 3% Nital. At low magnification, the fracture surfaces of each type of specimen exhibited different appearance, strongly affected by the welding pass orientation.

Table 3. The fracture toughness values measured on BxB and Bx2B specimens [5]

Specimen		a_o mm	a_o/W -	δ_i mm	F_i kN	$\delta_{c,u}$ mm	F_{ma} kN	Microstructure in a crack tip
Bx2B	Bx2B-1	35.180	0.49	0.045	101	0.079*	127.7	
with	Bx2B-2	35.410	0.49	0.066	115	0.085	126.5	
through	Bx2B-3	35.640	0.50	0.041	107	0.098	126.4	
thickness	Bx2B-4	34.310	0.48	0.061	116	0.117	145.9	
notch	Bx2B-5	35.230	0.49	0.065	113	0.123	137.8	
	Bx2B-6	35.850	0.50	0.104	121	0.118	123.4	
	BxB-rh-1	7.271	0.20	0.167	174	0.561	228.6	re-heated-1
	BxB-rh-2	10.135	0.28	0.168	153.2	0.405	182.1	re-heated-2
	BxB-rh-3	9.626	0.27	0.158	167	0.233	178.2	re-heated-3
BxB	BxB-rh-4	9.912	0.27	0.135	160	*0.228	173.6	re-heated-4
with	BxB-ad-1	10.200	0.28	*0.019	59.6	deffect	due	by pore-1
surfce	BxB-ad-2	9.791	0.27	0.045	106	0.102	102.1	as-deposited-2
notch	BxB-ad-3	9.654	0.27	0.046	88.9	*0.105	130.8	as-deposited-3
	BxB-ad-4	8.657	0.24	0.060	109	0.117	146.3	as-deposited-4
	BxB-ad-5	11.610	0.32	0.045	88.7	0.247	153.2	as-deposited-5
	BxB-ad-6	6.780	0.20	0.059	102.4	0.263	179.6	as-deposited-6
	BxB-ad-7	6.980	0.20	0.080	117	0.267	179.1	as-deposited-7
	BxB-ad-8	6.830	0.20	0.090	128	0.345	194.9	as-deposited-8

*-critical value *CTOD*(δ_c) at unstable crack growth or stable crack growth of less than 0.2 mm.

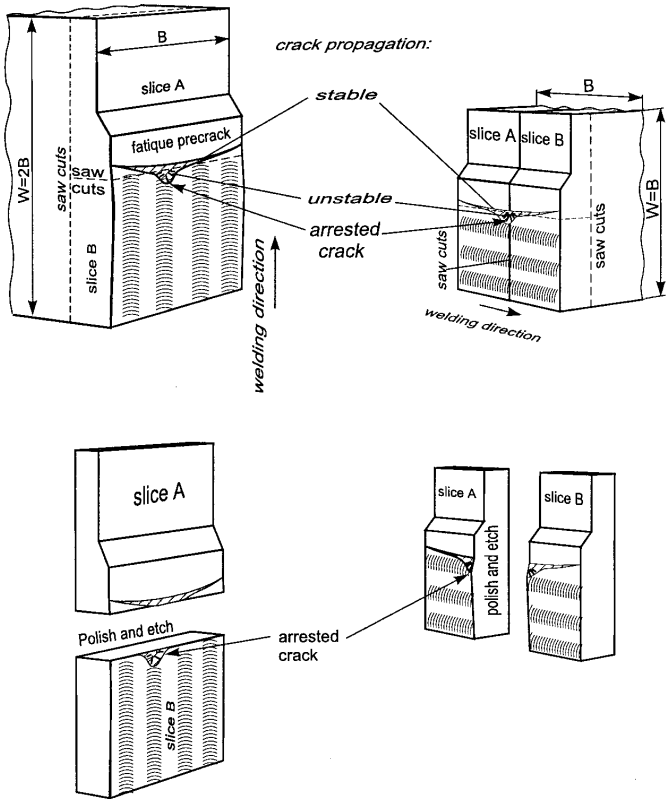

Fig. 3. Sectioning plan of tested specimens Bx2B and BxB

a) Through-thickness-cracked specimen (Bx2B)

Figure 4 shows the location of a through-thickness crack in the multi-pass welded joint, whereas the fracture surface appearance of a typical Bx2B specimen is shown in Figure 5. It can be seen in Figure 5, that the crack growth (small darker area in the upper part of Fig. 5) is accompanied by delimitation of the welding passes, which reduces resistance to crack growth. The corresponding force-CTOD curve is shown in Figure 6, exhibiting only insignificant pop-in step during linear loading. This pop-in was formed in the local soft region within the weld pass (Fig. 7). The next pop-in step, but a significant one, occurred after a certain amount of stable crack growth, Figure 6. The fracture surface of final instability was formed as a quasi-cleavage surface. This was confirmed by a fractographic examination of the fracture surface where several local brittle zones were surrounded by ductile fracture surfaces. The microhardness was measured along the contour of the fracture indicating that the pop-in crack was initiated at the end of the microstructure with higher hardness. The quasi-cleavage crack has propagated through the soft region (265 $HV_{0.1}$) and arrested in the medium hardness region (295 $HV_{0.1}$).

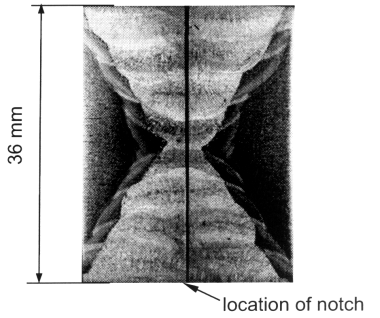

Fig. 4. Macro-etched photograph of specimen Bx2B, with crack tip in the weld metal centre

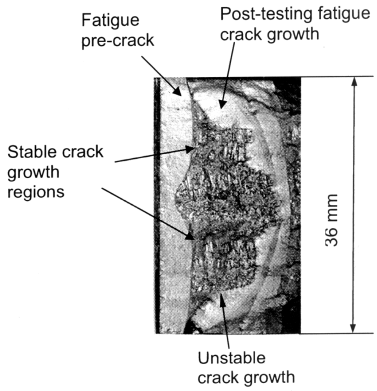

Fig. 5. Fracture surface of specimen Bx2B

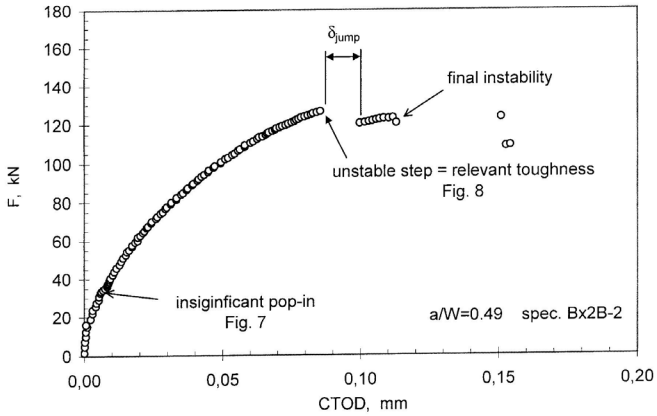

Fig. 6. F-CTOD(δ_5) curve recorded during fracture toughness testing Bx2B-2 specimen

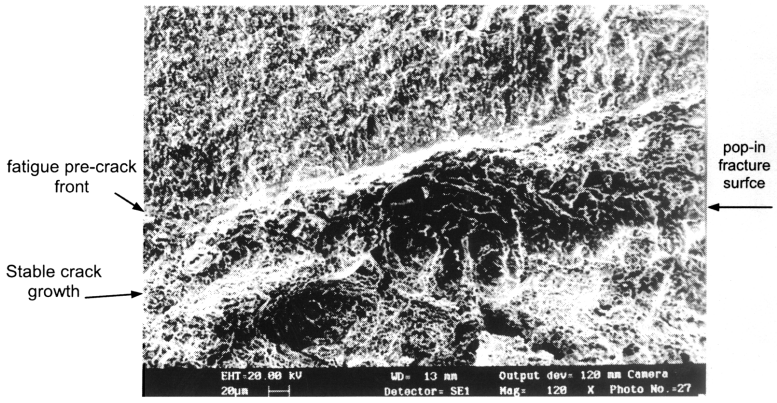

Fig. 7. Pop-in surface surrounded by ductile tearing region

b) Shallow-cracked specimen (BxB)

Figure 8 shows the whole crack propagation contour for the shallow-cracked specimen with crack tip in BxB-as-3 while the typical fracture surface is shown in Fig. 9.

Since the fatigue crack front is parallel to the welding direction, the fracture behaviour depends on the microstructure where the crack tip is located. Hence, surface notched specimens (BxB) with the same crack depth (a/W=const.) in regard to microstructure can exhibit high (re-heated) and low (as-welded) critical $CTOD_i$ values. Local unstable fracture behaviour ("pop-in") can also occur during stable crack propagation, where the crack tip crosses the low tough microstructure. It is obvious from Figure 10, where, from the same specimens and same crack depth, completely different fracture behaviour occurred.

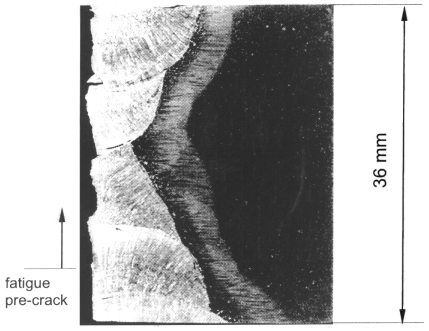

Fig. 8. Macro-etched photograph of specimen BxB-as-3, with surface notch tip in the weld metal

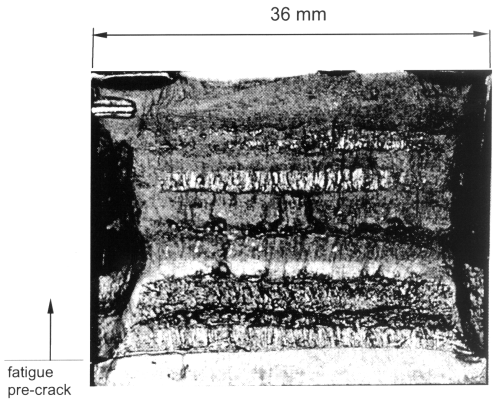

Fig. 9. Fracture surface of specimen BxB-as-3

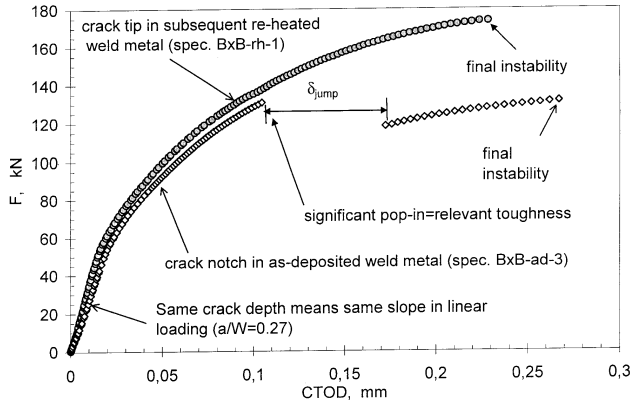

Fig. 10. F-CTOD curves recorded during fracture toughness testing BxB specimens

In order to compare the fracture behaviour of two specimens with the same depth of surface crack, but different microstructure at the crack tip, two typical loading curves (F-CTOD) are presented in Figure 12.

The loading curve for the specimen (BxB-10) with the crack-tip in as-welded columnar microstructure shows pop-in event. The significant pop-in step occurred below the linear loading when the crack tip was located in the as-deposited region. After the pop-in step and a certain amount of stable crack propagation and CTOD, final instability occurred.

The specimen (BxB-1) with the crack tip in the re-heated microstructure, exhibited stable crack propagation without pop-ins, Figure 12. Crack tip located in fine martensite with contours of primary ferrite (PF). The final instability was initiated by several origins along the front of the ductile crack growth, producing a quasi-cleavage fracture.

A further metallographic investigation was performed on a slice of the BxB specimen in the direction of crack propagation. Figure 11 suggests that the metallic inclusion from the flux core wire is the low toughness region in the weld metal, showing the obvious effect on any additional cracking. The electronic microanalyses showed that the content of Cr and Ni varied along the line A-A, Fig. 12. In the inclusion the content of Cr was 1% to 5%, while in the surrounding weld metal it was 0.9%. Similarly, the content of Ni also varied from 3.1% to 9.8% in the inclusion, while the grain otherwise contained 2.5%.

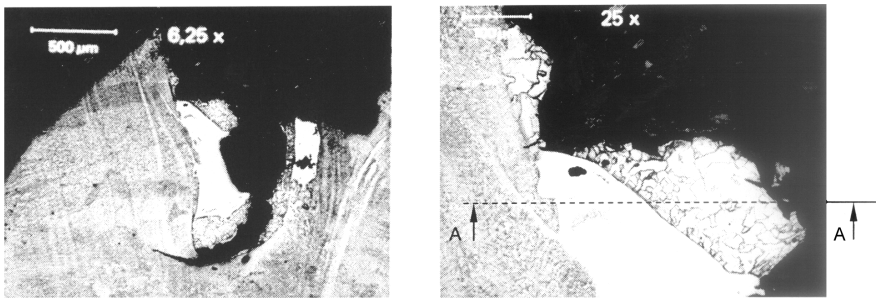

Fig. 11. Metallic inclusion at the vicinity of the cleavage crack propagation front

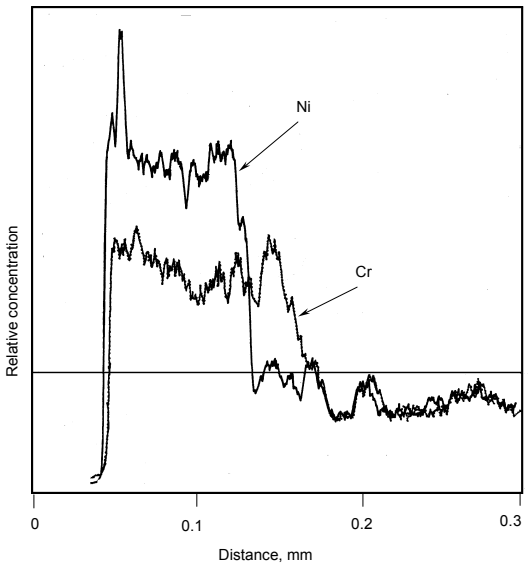

Fig. 12. Relative concentration of Ni and Cr in the metallic inclusion

In addition, the strip of pro-eutectoid ferrite can affect the secondary cracking emanating from the curved leading edge of the dominant crack, Figure 13. Metallographic analysis shows that the cleavage crack can easily propagate along the border of the pro-eutectoid ferrite, Figure 13.a). Thus, it is possible to conclude that the large austenitic grains, aligned by pro-eutectoid ferrite, were suspected of causing the crack propagation. An ESM analysis was performed on the strip of pro-eutectoid ferrite. The location of the path of the wave dispersion spectrometer-WDS beam path is shown in Figure 13.b). The analysis showed that pro-eutectic ferrite is poor with Cr and Ni, Figure 14 increasing the temperature of γ–α transformation and decreasing the strength at the same time.

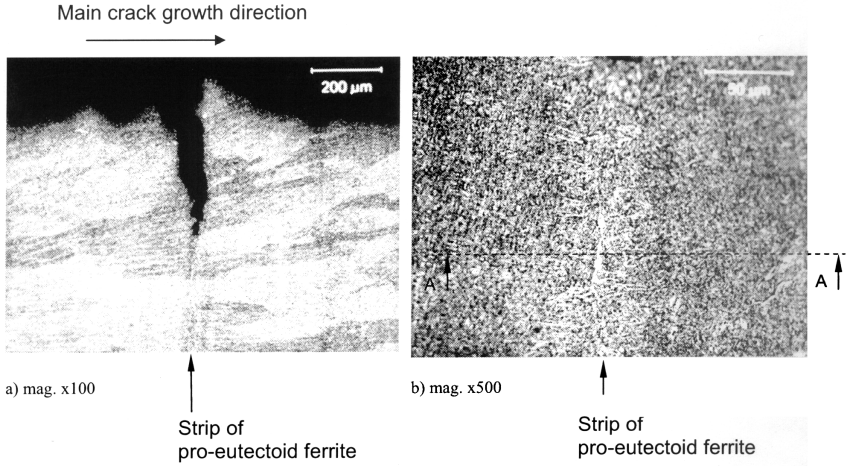

Fig. 13. Strip of proeutectoid ferrite perpendicular to the dendritic solidification in the weld metal

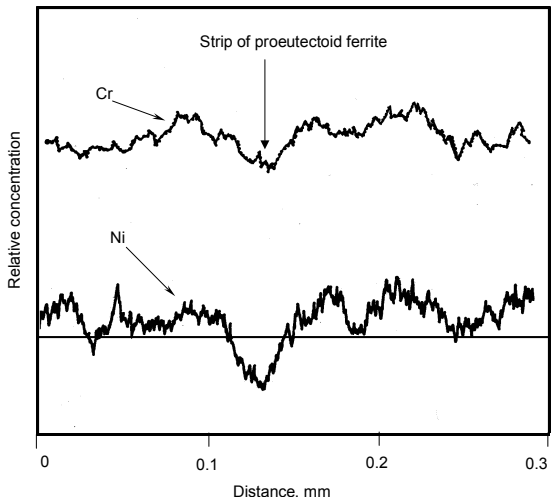

Fig. 14. Relative concentration of Ni and Cr in partially soluted proeutectoid ferrite

4. DISCUSSION

It was possible to recognize that the local brittle region in the weld metal was a region with lower hardness (240-270$HV_{0.1}$) from the microhardness measurements. The local instability occurred when the crack propagated from the hardened region (320-350$HV_{0.1}$) to the lower hardness region. The whole soft valley and as-deposited weld metal was brittle. The cleavage crack propagation was arrested in the reheated region of higher toughness.

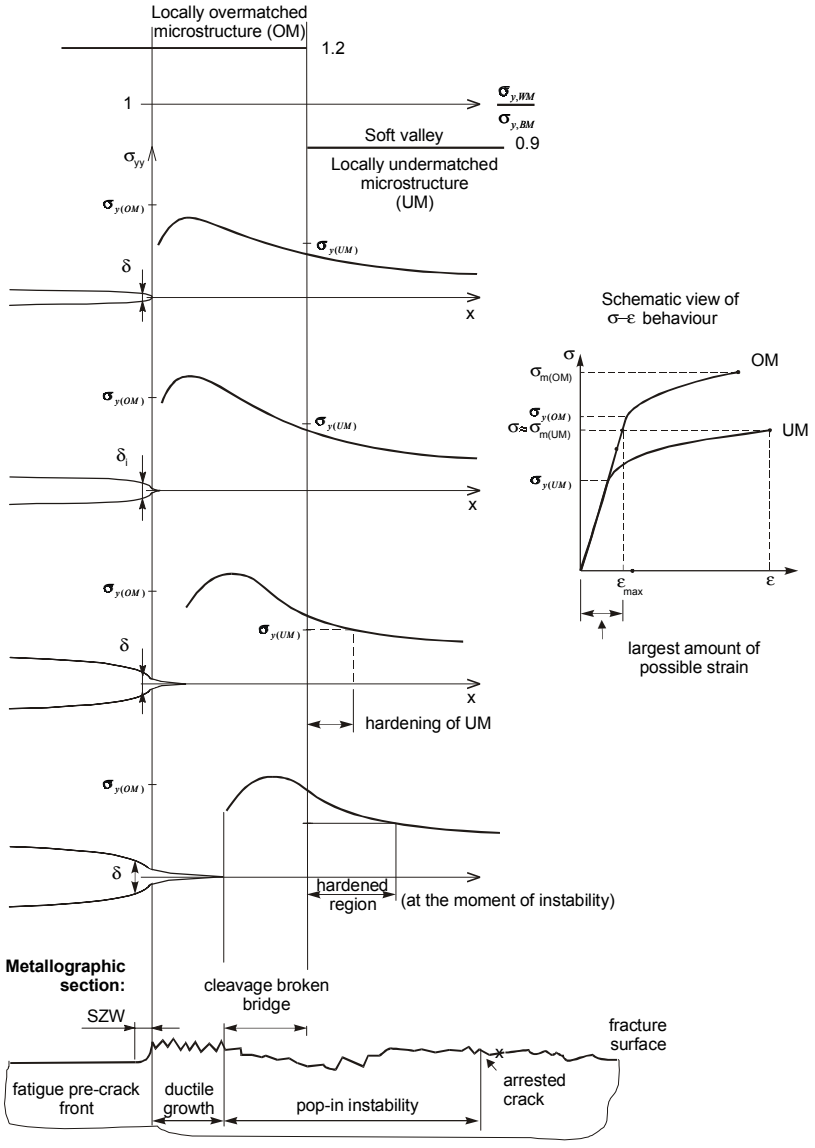

Fig. 15. Schematic presentation of fracture propagation through strength mis-matched microstructures

Figure 15 schematically illustrates fracture behaviour during crack propagation from the overmatched to the undermatched microstructures'. The crack tip was blunted in the overmatched region, creating a corresponding stress field. During the stable crack propagation the stress peak decreased slightly and shifted with the stable crack tip towards the undermatched microstructure. The overmatching stress field in the vicinity of the undermatched weld metal caused hardening of the undermatched microstructure. This happened prior to the crack tip coming into contact with the undermatched microstructure. The initiation of the cleavage fracture was caused by a critical level of hardening in the undermatched weld metal. The cleavage bridge was partly formed in the overmatched weld metal at the point of instability.

The described fracture behaviour always occurred when the stable crack propagated to the undermatched weld metal or the microstructure with lower toughness. In this case it is impossible to prevent pop-in step. As shown, other brittle microstructures involve metallic inclusions and pro-eutectoid ferrite. The effect of metallic inclusion depends strongly on their size, shape and hardness. In the case of inclusions like the one shown in Figure 13, the dominating effect is due to increased hardness and interaction with the surrounding weld metal, which then acts as a softer material according to the mechanism described in Figure 14. Nevertheless, in this case, the effect is local and not of the same importance as when different microstructures interact. On the other hand, the effect of pro-eutectoid ferrite has not involved the mechanism described in Figure 25, but rather the secondary cracking along the characteristic direction of microstructure, Figure 13.a) and b). The fact that pro-eutectoid ferrite has lower strength due to decreased content of Cr and Ni, does not produce the hardening effect because the primary stress field is uninvolved, i.e. this microstructure is not ahead of the crack tip.

5. CONCLUSIONS

This analysis of the unstable fracture behaviour of an overmatched weld metal has shown that a high strength material is extremely sensitive to the presence of strength mismatched local regions.

The overmatched weld metal exhibits an unstable crack propagation, whilst the base metal is ductile. Unstable crack propagation of a weld metal is affected by:

a) local strength mis-matched microstructures,
b) direction of crack propagation

The local strength mis-match within a weld metal is affected by the presence of:

a) local soft region tempered between Ac_1 and self-tempering temperature.
b) partly solid metallic inclusions with higher contents of alloying elements
c) pro-eutectoid ferrite

Local strength mis-match localized the yielding and strain hardening in the undermatched region of the weld metal, contributing significantly to unstable fracture behaviour.

The direction of crack propagation relating to the sequence of welding passes also affects fracture behaviour. In the case of the shallow-cracked specimens, fracture behaviour is affected by the position of the crack tip. If the crack tip is in the re-heated microstructure then ductile crack propagation can occur with or without insignificant

pop-in. If the crack tip is located in the as-deposited microstructure the pop-in unstable step or unstable fracture behaviour is commonly exhibited. Thus, a significantly different range of experimental results can be obtained. In the cases of specimens with through-the-thickness cracks, the range is significantly lower, but also the toughness itself. The arrest of the unstable crack growth is not only the consequence of a load drop, but the presence of a microstructure where the crack tip is arrested. Structural integrity is possible to ensure not only by an appropriate structure assessment integrity procedure, but also by considering elements which threaten the sage service of the overmatched welded joint. Consumables for high strength overmatching welded joints (yielding above 700 MPa) are subjected to local brittle zones. Therefore, such a weld joint requires metallographic analysis as explanation of the experimentally obtained fracture behaviour.

REFERENCES

1. Gubeljak N.: "Fracture behaviour of specimens with surface notch tip in the heat affected zone (HAZ) of strength mis-matched welded joints. *Int. j. fract.*, Dec. 1999, vol. 100, issue 2, pp. 155-167.
2. Defourny J.: *"Guide to Weldability and Metallurgy of Welding of Steels Processed by Thermomechanical Rolling or by Accelerated Cooling",* IIW Doc. IX-1649-91 and IXA-32-91
3. Vojvodic-Tuma, J.*: "Determination of Lower Bound Fracture Toughness of the Overmatched Weld Metal of High Strength Low Alloy Steel",* submitted to journal Engineering Fracture Mechanics, 2002.
4. "*Compendium of Weld Metal Microstructures and Properties (Submerged-arc Welds in Ferritic Steel)",* Prepared for Commission IX of the International Institute of Welding by Sub-Commission IXJ, The Welding Institute Abington Hall, Cambridge UK 1985#
5. BS 7448: Part 2: 1997: *Fracture mechanics toughness test, Part 2. Method for determination of K_{Ic}, critical CTOD and critical J values of welds in metallic materials*, British standards institution, London, 1997
6. Gubeljak N., Legat, J., Koçak, M.:"*Effect of Fracture Path on Toughness of Weld Metal*", to submitted in International Journal of Fracture, 2002

NESTABILNO LOMNO PONAŠANJE METALA ŠAVA KOD NISKOLEGIRANOG ČELIKA POVIŠENE ČVRSTOĆE

Nenad Gubeljak

Lokalno krhka područja (LKP) uzrokuju nestabilno lomno ponašanje metala šava. LKP time ugrožavaju sigurnu eksploataciju zavarene konstrukcije, a procena integriteta konstrukcije postaje zahtevnija. Zbog toga je potrebno detaljnije istražiti uzrok nestabilnom lomu metala šava kod niskolegiranog čelika povišene čvrstoće. Istraživanja su pokazala, da interakcija izmedju dve mikrostrukture metala šava s različitim ojačavanjem može prouzrokovati nastanak LKP, koje uzrokuje nestabilno lomno ponašanje. Oblikovanje područja niske čvrstoće i tvrdoće u metalu šava s više prolaza je posledica ponovnog segrevanja na temperature izmedju Ac_1 i temperature samopopuštanja. Prisutnost delimično stvrdjenih metalnih uključaka s visokim postotkom legirnih elemenata i pro-eutektičkog ferita može biti dodatan uzrok za lokalno nestabilno lomno ponašanje metala šava. Spomenuta područja karakteriše bitno niža granica tečenja s različitim deformacijskim ojačavanjem u metalu šava globalno visoke čvrstoće, što može dodatno prouzrokovati nestabilno lomno ponašanje metala šava. Istraživanja su pokazala da je to jedan od ključnih elemenata koji prouzrokuju rasipanje eksperimentalnih rezultata kao što je kritična vrednost parametra lomne žilavosti, kad se prslina širi iz jedne zavarenog prolaza prema drugom. U slučaju lomnomehaničkih ispitivanja s prsilnom kroz više zavarenih prolaza istovremeno (prislina prolazi kroz debljinu celog spoja) je rasipanje rezultata uz opšte nisku žilavost mnogo manje.